

Free-Form Grid Structure Multi-Objective Optimization Associated with Integrated Design and Machine Learning

Mahdi S. Fard (✉ m.soheylifard@gmail.com)

Ardaena.com

Elham Ghaderi

Shahid Rajaee Teacher Training University

Mohammad Pour Fooladi

Polytechnic of Milan

Research Article

Keywords: Integrated Design, Grid structures, Multi-Objective Optimization, Machine Learning, Clustering

Posted Date: October 18th, 2023

DOI: <https://doi.org/10.21203/rs.3.rs-3439064/v1>

License:   This work is licensed under a Creative Commons Attribution 4.0 International License.

[Read Full License](#)

Additional Declarations: No competing interests reported.

Free-Form Grid Structure Multi-Objective Optimization Associated with Integrated Design and Machine Learning

Mahdi S. Fard ¹[0009-0005-3063-659X] Elham Ghaderi ²[0009-0002-5645-8291]
Mohammad Pourfouladi ³[0009-0009-7255-2983]

¹ Independent Researcher, Ardaena.com, Qom, Iran

² Shahid Rajaee Teacher Training University, Tehran, Iran

³ Polytechnic of Milan, Milan, Italy

m.soheylifard@gmail.com

Abstract. Grid structures are among the lightest spatial structures for supporting large-span shells while constructing an efficient free-form casefree-form is exceedingly challenging. This research aims to investigate a special type of pattern for free-form grid structures using a process that combines selected design variables with their corresponding structural properties. Therefore, functional grid structures based on traditional Iranian geometries are parametrically interconnected in a workflow, where the results are compared to a base case. Iranian Chahar-Lengeh Girih as the main generative designer is generated by the Hankin Method that defines a controlling parameter (P) for the shape typology where the elements of the structure support a simple quadrilateral grid or a reciprocal one. Comparing these two validates the structural efficiency of architectural and structural performance. The workflow carries out a multi-objective evolutionary algorithm (NSGAI) to optimize the structural performance of the free-form grid structures with satisfying the architectural design requirements concomitantly. It is composed of the design-related part which includes the parameters of generating free-form grid structures, while the element diameter, element thickness, and the number of columns represents the structure-related counterparts. Consequently, reducing Mass, Displacement, and Elastic Energy are optimization objectives, besides K-Means Clustering with diverse approaches is used to explore patterns of possible solutions among the functions. The results portray that in the Overall-Best solution extracted by the workflow, with a P parameter equal to 0.8, Displacement, and Elastic Energy are improved by %88.44 and %89.82, respectively compared to its Reference Case where P = 0.5 (simple grid shell).

Keywords: Integrated Design, Grid structures, Multi-Objective Optimization, Machine Learning, Clustering

Statements and Declarations

- **Acknowledgement and Funding**
No funding was received for conducting this study
- **Competing Interests**
The authors have no relevant financial or non-financial interests to disclose.

1 Introduction

The free-form grid structure has been widely used in spatial structure development due to its architectural expression. Traditional grid structures usually have simple shapes and regular grids. Computational modeling has made it possible to create free-form grid structures with complex shapes and grids in spatial structures. Also, structural optimization provides novel ideas for the computational shape generation of structures [1]–[3]. In related research projects that address optimization, structural weight is often one of the primary objective functions. The geometrical values and the cross-sectional shape of the elements are commonly considered as Design Variables for implementing the computational workflows to be applied for optimization [4]. The inclinations in such projects are commonly set toward form optimization [5]–[9], elements' size optimization [10] and topology optimization [11]. Since it is not always explicit how to create an efficient grid pattern in free-form by integrating selected DVs with responding to structural variables; therefore, most have studied regular shapes, such as triangular or quadrangular grids, or a combination of basic paneling patterns [12], [13]. Although in recent years, more creative grids, such as hexagonal and polyhedron grids, have been developed by researchers [14] that address the more flexibility that can be offered by architectural aspects, the greater optimized structural forms are expected.

Nomenclature

<i>MOEA</i>	<i>Multi-Objective Evolutionary Algorithm</i>
<i>MOGA</i>	<i>Multi-Objective Genetic Algorithm</i>
<i>NSGA</i>	<i>Non-Dominated Sorting Genetic Algorithm</i>
<i>MOO</i>	<i>Multi-Objective Optimization</i>
<i>SOO</i>	<i>Single-Objective Optimization</i>
<i>GA</i>	<i>Genetic Algorithm</i>
<i>DVs</i>	<i>Design Variables</i>
<i>PCA</i>	<i>Principal Component Analysis</i>
<i>ML</i>	<i>Machine Learning</i>
<i>BO</i>	<i>Best Overall</i>
<i>BD</i>	<i>Best Displacement</i>
<i>BEE</i>	<i>Best Elastic Energy</i>
<i>BM</i>	<i>Best Mass</i>

Several researchers have depicted that it is not always obvious how to create an efficient grid shell structure when it comes to free-forms. Designers face a challenging process when selecting the optimal pattern and geometry for a grid in order to achieve additional structural efficiencies. Many research projects have focused on optimizing free-form grid structures using single and Multi-Objective Optimization in order to achieve this efficiency and in such endeavors, MOO problems have been extensively studied using evolutionary algorithms. Different Multi-Objective Evolutionary Algorithms have also

been projected for this purpose and one of the most common is the Non-Dominated Sorting Genetic Algorithm (NSGA-II) [15]. The subsequent paragraph discourses some

of the research projects using NSGA-II since the algorithm has been introduced by Professor Deb et al. in 2002.

Several studies [4], [16]–[24] represent the importance of NSGA-II for working with the variant design process. Among the significant ones, there is the presentation of a method for the synthesis of optimal grid structures using MOO with NSGA-II [18]. Such attempts are followed by Richardson and others representing a novel yet general approach to grid shell structure preliminary design which uses a combination of form-finding with grid configuration correlated with GA optimization techniques [20]. These research outputs mostly correspond to substantial mass reduction by optimizing the grid shell configuration in paneling shape and form. Developing such already approved methods is possible to have geometrical variables added to the problem formulation.

The MOO of free-form cable-braced grid shells was examined by Feng et al in 2015 to support the feasibility of this perspective. Multi-objective indices are employed in this case, including mechanical properties indexes (maximum displacement, buckling loads, strain energies), geometrical indexes (mean square deviation of tube lengths, a difference between the optimal surface and the initial surface), and economic indexes (strength of the tubes). Succeedingly, a new MOO procedure was developed by Ehsani and Dalir in 2020 to determine the grid plate's architecture (pattern and geometry). This model is called the variable rib model (VRM) written for GA and uses ϵ -constraint approach. In the ϵ -constraint method, only one of the objectives gets optimized during the optimization process. A similar study by Goodarzi et al in 2023 examines the effect of collaboration between structural and architectural features on improving grid shell efficiency on non-regular surfaces with a MOO algorithm designed to minimize displacement and steel weight which clinches the possibility of linking different parameters to a specific feature.

According to this study, minimizing displacement, and elastic energy, among the mechanical properties, and minimizing the structure's weight, among the economic attributes, have been identified as three important objectives in the optimization of grid shells. Furthermore, since minimizing one item may negatively impact the others, this research proposes a MOO approach to manage the true proportion among objective functions. Although The optimization of the pattern and geometries of the grid structure has also been the subject of numerous studies, reaching a multidisciplinary method that integrates architecture and structure in the free-form grid structures through the relationships between them is the problem; This could contribute to the definition of free-form grid structures that, along with the appropriate form and pattern, have also reached a balance in terms of structural elements. Consequently, the preferences behind this research are established by answering the following question:

- How an optimization setting can offer a free-form grid structure with proper form, pattern, and balanced structural components?

Using MOO algorithms is a crucial part of this study in respond to the question. One of the most widely used algorithms in this area is NSGA-II which provides editing of the definitions and accelerates the process in accordance with the objective types and functions. By using this framework to improving the structural features integration of a freeform grid structure, this study aims to maximize the benefits of architectural DVs while enhancing their structural performance. While using this method, a set of optimum dimensions is obtained for the grid structure. This allows the workflow to be set up for the determination of the optimal pattern and minimization of displacement, elastic energy, and mass. There are two sets of variables involved in the optimization process. As part of the design component, parameters are provided for generating a grid shell based on free-form and structural patterns. Regarding that, this research employs the Hankin method to draw a Chahar-Lengeh Girih for generating a reciprocal pattern. In addition, structure-related parameters include the element and column diameters, their thicknesses, and the number of columns. The dataset integration checkpoints are investigated using K-Means clustering algorithms amplified by Principal Component Analysis (PCA) to reduce cluster variation dimensions due to the large number of variables in this study. In addition, the clusters are visualized to demonstrate their characteristics concerning design and structural variables.

2 Research Methodology

Architects design only based on general knowledge and structural conceptual concern without evaluating the optimal performance of free-form grid structures. For this purpose, to achieve the optimal grid structure by integrating parameters from design to structure, MOO algorithms must involve searching for solutions that optimize two or more conflicting objectives, such as minimizing cost while maximizing performance. Research involving MOO requires a workflow that integrates parameters with various factors, from design through analysis to optimal results, ensuring all relevant information is considered during optimization.

In this study, a comprehensive approach was used to identify patterns that can be used to optimize design decisions through feature-based iterations, allowing MOO algorithms to achieve better results. As a result, a customized workflow is established that integrates data from multiple sources, including design parameters, structural analysis, and results. Parametric modeling and structural analysis are uniquely constructed. Thus, in order to understand the aforementioned characteristics, it is necessary to investigate the variables that comprise a free-form grid structure and their relationship with the structure of the form. Accordingly, the factors that comprise the parameters of generating a free-form grid structure, such as the coordinates of the points forming the free-form, and Girih creator parameter, as well as additional variables that can be eval-

uated, such as element diameter, element thickness, and a number of columns, are examined in this study. In **Fig. 1**, inputs, layers of analysis that are applied by MOO using NSGA-II, Machine Learning (ML), and outputs are indicated in a flowchart.

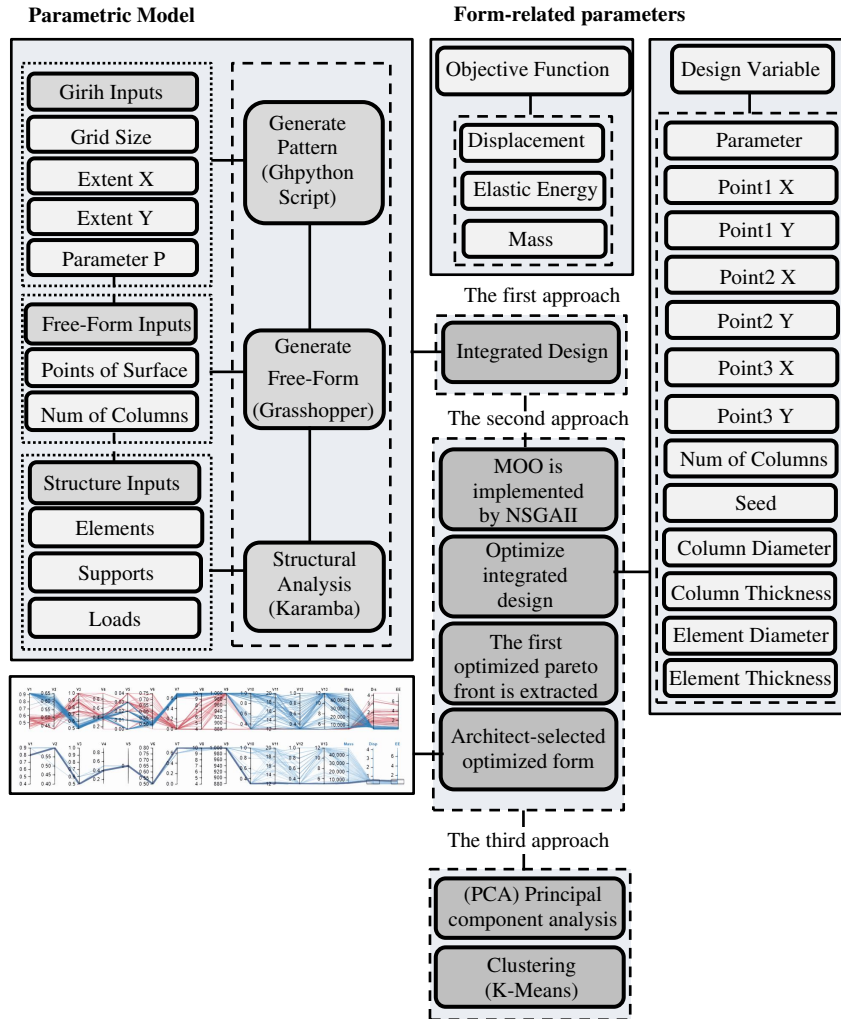


Fig. 1. Flowchart of the process of analysis and optimization

In the first segment of the research, Girih Geometry while highlighting a structural pattern that controls force flows by reciprocal interactions; should be constructed for analyzing structure. Since part of the design relies on the Girih pattern, the primary parameter called p, for generating a diverse format, represents the Girih Parameter in the 0.00:1.00 domain. In order to maintain asymmetrical properties, a free-form structure needs to have adapted support positions. Furthermore, parametric randomization

is used in this section to produce a more performable location. Python programming language enhanced this setup besides using Grasshopper to fulfill the algorithm's input-to-output setting.

In the second step, Once the model generator setup was established, the analysis part was organized using Karamba3D [25] to determine the particular objectives: Mass, Displacement, and Elastic Energy. To converge and decrease these three objectives, the DVs have been extensively updated and extended during the iterative generating process. This phase, known as generative design, enables the generation of an endless number of design choices within a wide solution yet adaptable design space. This process is accomplished by repeating the loop through Multi-Objective GA implemented in Jupyter Notebook. The Pareto-optimal solutions in this section represent the best possible alternatives for the design section's grid structure. Finally (selection stage), The best design options resulting from the optimization part were extracted, and the chosen one solution was selected according to the architect's priorities and project conditions using the Design Explorer online platform [26].

In the third phase, following the construction of the dataset, a 100×16 matrix is used for Clustering. The recorded data was transferred to Jupyter Notebook for applying K-Means Clustering, one of the most common techniques for clustering numeric data [27], and PCA, [28]. to reduce dimensions through comprehensive elongations and reflections on each design iteration. The following paragraphs describe each study step and its associated practical instruments in depth.

2.1 Step 1: Parametric Design and Generation

Pattern Generation

Implementing the framework for form-finding begins with generating a structural pattern from which the grid shell can be derived. According to this study, Islamic geometric patterns were selected based on the need to use a linear model to analyze structural

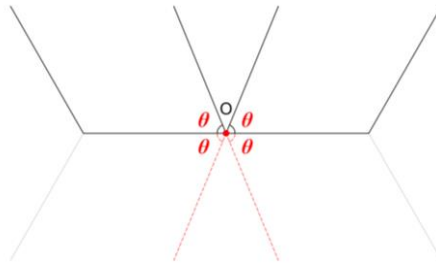


Fig. 2. The x-shaped lines are in the middle of the sides of the polygon, each with a certain angle of incidence to the sides of the polygon. (Drawn by authors)

performance and to achieve more flexibility in grid structure patterns from the architectural perspective. In adaptive geometric grammars, these patterns serve as reciprocal elements.

The approach that addressed how to produce and develop Islamic geometric patterns in the West was first introduced in articles by Hankin under the titles of “The Drawing of Geometric Patterns in Saracenic Art”, “Examples of methods of drawing geometrical arabesque Patterns” and “Some difficult Saracenic designs”[29]–[31].

Hankin first presented the method of the guide network of polygons in the article “The Drawing of Geometric Patterns in Saracenic Art”. His description of this technique provides a starting point for an algorithmic approach. He pointed out that covering a surface with a polygonal grid is necessary for making such patterns. Then, two lines are drawn through each of the edges of the polygons. These lines cross each other like an x and continue until they reach similar lines passing through other edges [29]. A key variable in the model is the collision angle between the outwardly extending edges and polygon edges. (See **Fig. 3**). Also, **Fig. 2**, shows Different results can be created by changing the angle using Hankin’s method [32].

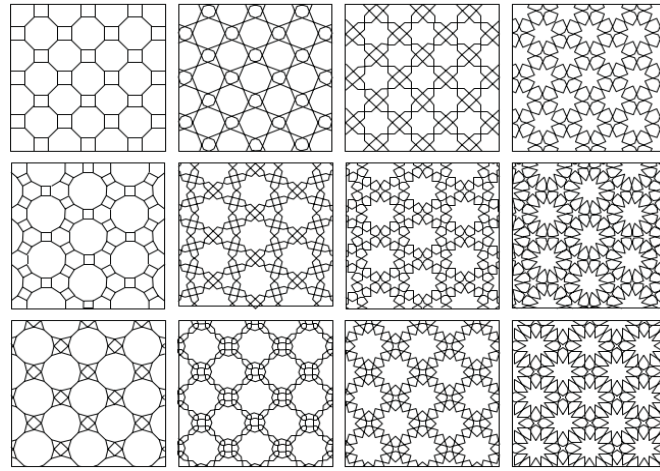


Fig. 3. Different results by changing the angle using Hankin’s method

Based on several case study reviews, the Char-lange or Chahar-lengeh or Hasht-va-chahr-lengeh Girih [33], which are relatively widely used in Iranian geometries in wooden works among Islamic geometric patterns, was selected respecting to the following features it has (see **Fig. 4**). A distinctive characteristic of this Girih is having this ability to adapt itself to the Hankin method as well as its quadrilateral fitness within a guiding grid. In this manner, it becomes easier to match the grid to a quadrilateral mesh, thus simplifying geometrical design. In addition, it can also be adjusted to any angle, and it is capable of supporting intricate and complex design processes by defining specific variables.



Fig. 4. Chahar-lengeh Girih from the stair fence of the minbar in Nain Mosque

To drawing a Chahar-lengeh Girih followed traditional instructions, the first step is to draw a square (ABCD) and its diameter. The second step is to draw circles from each vertex of the square with a radius of half of the side edge. The adaptable points E, F, G, and H are located where the arcs of circles meet the AC and DB lines. Additionally, the last step is to connect adaptable points to the middle of the square edges respectively (see **Fig. 5**).

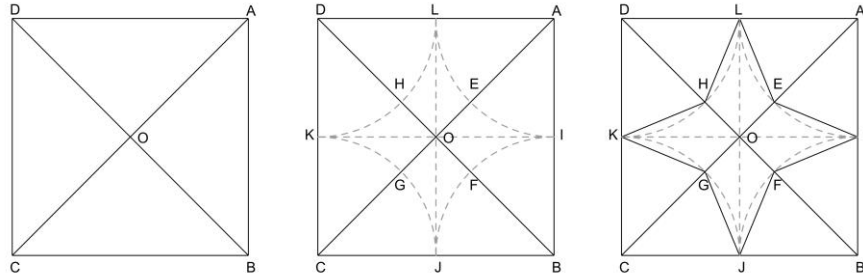


Fig. 5. The traditional method of drawing a quadrilateral knot described

The geometric pattern drawn in the traditional way forms an angle of 67.5 degrees at the intersection of the side edges and the reciprocal lines (angle θ). In Hankin's method, different shapes are created by changing the angle θ , considering the fact that the study looks to determine the length of the components and compare them in each performative exploration; therefore, it is preferred to define a numerical parameter (parameter p).

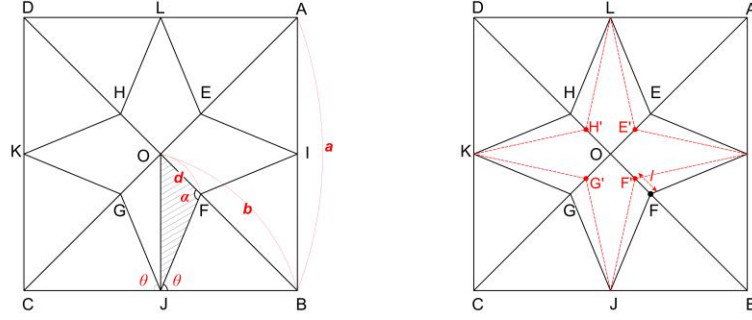


Fig. 6. The relationship between theta and parameter p

To get the relationship between theta and parameter p (see **Fig. 6**), which is the ratio of the distance between the reciprocal x-like lines and the center of the square(d) over the half diameter of it (b), the relationship of sines in the OFJ triangle in the left figure can precisely be established, referred to the following equations:

$$\alpha = 45 + \theta, \quad OJ = \frac{a}{2} \rightarrow \frac{\frac{a}{2}}{\sin(45 + \theta)} = \frac{d}{\sin(90 - \theta)} \rightarrow \frac{d}{a} = \frac{\cos \theta}{2 \sin(45 + \theta)} \quad (1)$$

$$p = \frac{d}{b}, \quad b = \frac{a}{\sqrt{2}} \rightarrow p = \frac{\sqrt{2} \cos \theta}{2 \sin(45 + \theta)} \quad (2)$$

Also, to compare the length of the components as shown in the right figure, by changing the p-parameter from p1 to p2 or in other words compare two star-shapes, LEIFJGJH, and LE'IF'JG'JH', the intersection points are moved by l (for example from F to F'), therefore:

$$p2 - p1 = \frac{OF'}{OB} - \frac{OF}{OB} = \frac{l}{b} \quad (3)$$

After introducing the Girih drawing method, its parametric design process was implemented by Python programming language enhanced by Grasshopper3D. It was intended to use this pattern as a design for a freeform structure in the form of a grid shell. For this purpose, parameters related to geometrical attributes and architectural design, such as the dimensions and number of squares (which are obtained by putting together a Cha-har-Lengeh Girih module) as well as the P parameter with the inputs affecting the structure, for example the attraction points defining the free-form shell and the minimum and maximum height of the structure was integrated so that the design and engineering factors of the structure can be examined in an unified way. This process has been conceptualized by Algorithm 1.

Algorithm 1 Parametric Design Workflow

```

1: procedure NAME (Form generating)
2:   P parameter  $\leftarrow$  define (Design Variables)
3:   grid size  $\leftarrow$  define (Design Variables)
4:   extent X  $\leftarrow$  define (Design Variables)
5:   extent Y  $\leftarrow$  define (Design Variables)
6:   function  $F_1$  ( P parameter, grid size, extent X, extent Y)
7:     Set a grid of squares with extent X and extent Y
8:     Set Squares' side lengths to grid size
9:     for loop
10:      Draw the diameters of each square
11:      Draw a line from the p part of half of each diameter
        to the midpoint of the adjacent sides of the square
12:      return lines, squares
13:   end function
14:   pt1, pt2, pt3  $\leftarrow$  define (attractor points)
15:   h1  $\leftarrow$  define (surface maximum height)
16:   h2  $\leftarrow$  define (surface minimum height)
17:   function  $F_2$  ( pt1, pt2, pt3, lines, squares, h1, h2)
18:     for loop
19:      Calculate each square center point
20:      Calculate the minimum distance between pt1, pt2, pt3 and each center
21:      Remap distances between h1 and h2
22:      Move centers with distances
23:     Create a surface with moved centers
24:     Map lines and square edges to the surface
25:     return lines, square edges
26:   end function
27: end procedure

```

Structural Analysis

Having defined the design and analysis process, an iterative free-form generator is established at this stage. To evaluate and explore the most optimal design(s), Karamba3D is utilized. Thus, interconnected parameters were defined so that the features of every design iteration can be studied with the structural analysis in parallel. These parameters are the number and position of the columns, the diameters, and thickness of structural elements, and the type of cross-sections each element obtains. In addition, Load Cases are defined accordingly. After carrying out the structural simulation, Maximum Displacement, Elastic Energy, and Mass were outputted in order to select the most optimal solution in the GA process. (See Algorithm 2)

Algorithm 2 Structural Analysis

```

1: procedure NAME (Structural analysis)
2:   N ← define (number of columns)
3:   Seed ← define (columns' positions)
4:   ED ← define (Elements Diameter (cm))
5:   ET ← define (Elements Thickness (cm))
6:   CD ← define (Columns Diameter (cm))
7:   CT ← define (Columns Thickness (cm))
8:   Main Load = 150 kg/m2
9:   Set support types
10:  Set cross-section type
11:  Set material
12:  lines ← define (elements and columns)
13:  function F1 (N, Seed, ED, ET, CD, CT)
14:    Run simulation engine
15:    Read the required constants
16:    Calculate the Maximum displacement, Elastic Energy
17:    Calculate the Mass
18:    return Maximum Displacement, Elastic Energy, Mass
19:  end function
20: end procedure

```

2.2 Step 2: Optimization and Evaluation**Multi-Objective Optimization Definition**

Engineers and architects may determine optimal solutions for complex problems by using the rule of optimization. In the engineering industry, derivatives are frequently used to solve variant numerical problems; however, in the field of architecture, resolving is much more complicated, and models include a wide range of independent and dependent variables entangled with objective functions from different influential factors. Therefore, such approaches like gradient descent are not reliable, because scanning the entire space involves expenditures of time and cost. Due to the large exploration data provided by parametric design, using a meta-heuristic approach to get to the optimal model is applied.

In order to match structural and architectural performance by considering a variety of structural parameters as well as form findings, the need for meta-heuristic algorithms, and continuous space exploration, it has been demonstrated that the GA Pareto front can be an effective method of achieving this objective. This paper considers thirteen DVs to form the design space. The variables and their variation domains are presented in **Table 1**. Also, the research method has been determined upon finding an optimum design space for grid structures to reach the cases with minimum Displacement, Elastic Energy, and Mass. This interconnected targeting that encompasses variables with true impact on the selection procedure in optimization models is termed the fitness objective setting. When a model contains more than two fitness objectives, it is called a multi-optimization model. Mostly, there is no single solution for MOO problems. Based on the application and situation, a designer decides which objective has priority over the others. The availability of an optimum design space for a grid structure helps to conclude a more certain combination setup of objectives for a particular prob-

lem. By integrating parameters from the design to the structural range, MOEA is employed to develop the optimal grid structure. A well-known and powerful MOEA, the NSGA-II algorithm, was also implemented and edited in Python in accord with the objectives.

Table 1. The Design Variables and their variation domains

Symbols	Description	Minimum Value	Maximum Value
X1	Parameter P	0.08	0.92
X2	Point1 X	0.00	1.00
X3	Point1 Y	0.00	1.00
X4	Point2 X	0.00	1.00
X5	Point2 Y	0.00	1.00
X6	Point3 X	0.00	1.00
X7	Point3 Y	0.00	1.00
X8	Number of Columns	4	10
X9	Seed	0	1000
X10	Column Diameter	0.30	1.00
X11	Column Thickness	12.00	20.00
X12	Element Diameter	0.30	1.00
X13	Element Thickness	5.00	12.00

To apply NSGA-II, a specific guideline has been developed for constructing algorithms, and hyperparameters must be set up according to the hardware requirements. The first hyperparameter is the population, so the population for the first generation was chosen consonantly. The second parameter needs to be set is Crossover. After the initial population started generating at random, the GA used this procedure to produce offspring. At first, this population mate in pairs.

$$if \rightarrow (V_1, U_1) \& (V_2, U_2) \rightarrow (\frac{V_1, V_2}{2}, \frac{U_1, U_2}{2}) \quad (4)$$

After producing an offspring, the procedure is followed by adding population and offspring information to the list before selecting the optimal Pareto front. This loop is repeated multiple times until the optimal Pareto front is found. However, the algorithm sometimes finds a local rather than global optimum. Because of this, scientists employ mutations in each generation to randomly scan the entire space.

$$Data \rightarrow (Population + offspring + mutation) \quad (5)$$

Throughout the process, Crowding Distance has been used to determine the optimal solution among information in which there is no consensus. The resulting moves are not capable of determining an optimal solution, regardless of how far they go. These conditions are necessary for dominating d1 to d2, which represent cardinally based solution sets and their distances from solution boundaries. In the first condition, all functions in d1 must be smaller or equal to d2, this condition is necessary but is not sufficient for Eq. (6).

$$\begin{cases} d_1 = \{f_1^{d_1}, f_2^{d_1}\} \\ d_2 = \{f_1^{d_2}, f_2^{d_2}\} \end{cases} d_1 \text{ dom } d_2 \rightarrow \text{allData} \rightarrow \forall_i f_i^{d_1} \leq_i f_i^{d_2} \quad (6)$$

The second prerequisite is the existence of an i such that the first structure's functions must be smaller than those of the second structure Eq. (7).

$$\text{any} \rightarrow \exists_i : f_i^{d_1} < f_i^{d_2} \quad (7)$$

All crowding distance must be gathered in this case, and among all Pareto fronts, the one with the greatest crowding distance wins Eq. (8).

$$\begin{cases} cd_i^1 = \frac{|f_1^{i+1} + f_1^{i-1}|}{f_1^{max} + f_1^{min}} \\ cd_i^1 = \frac{|f_2^{i+1} + f_2^{i-1}|}{f_2^{max} + f_2^{min}} \end{cases} \quad (8)$$

On the basis of the maximum crowded distance, the Data Eq. (5) will be sorted, and the best data will be selected [34]. The hyperparameters are set up generally including the number of Generation, according to population size = 100, the number of Crossover = 70, and the number of Mutation = 20. The hyperparameter of the alpha factor in the crossover was equal to 0.5, and the hyperparameter of the beta factor in mutation was considered equal to 10 of the ranges among the variables. Based on the algorithm and designer's experience, these settings for the algorithmic process besides defining the hyperparameters are chosen to enable exploration and exploitation, in a suitable equilibrium, lead to escape from the local optimum Pareto and ultimately identify the global optimum Pareto. The GA Pareto front's pseudo-code is illustrated in Algorithm 3.

Algorithm 3 NSGA II

```

1: procedure NAME (Calculate the optimal Parto)
2:   Initialize  $P0$  of candidate solutions
3:   Set  $P0 = (f1, f2, \dots)$  = non-dominated-sorted ( $P0$ ) for all  $fi \in P0$ 
4:   Crowding distance assignment ( $fi$ )
5:   Set  $t = 0$ 
6:   While not (termination criterion)
7:     Use a recombination method to create children  $Ct$  from  $Pt$ 
8:     Set  $Rt = Pt \cup Ct$ 
9:     Set  $f = (f1, f2, \dots)$  = non-dominated-sorted ( $Rt$ )
10:    Set  $Pt + 1 = \emptyset$ 
11:    Set  $i = 1$ 
12:    While  $|Pt + 1| + |fi| < N$ 
13:      Crowding distance assignment ( $fi$ )
14:      Set  $Pt + 1 = Pt + 1 \cup fi$ 
15:      Set  $i = i + 1$ 
16:    Do non-dominated-sorting with crowding distance to rank the individuals
17:    Set  $Pt + 1 = Pt + 1 \cup fi[1:(N - |Pt + 1|)]$ 
18:    Set  $t = t + 1$ 
19:    Return  $f1$ 
20: end procedure

```

2.3 Step 3: Clustering and PCA

Based on the last correlation among parameters included in each iteration, the study extended to identify more advanced connections between feature-based design scenarios. Thus, the recorded dataset was sent off to be analyzed using K-Means clustering to determine similar results in separate branches. The characteristics of the clusters are then explained by visualizing the clusters. The first stage comprises examining the Pareto front solution based on two objective functions (Displacement and Mass) as well as two important features for clustering which are the P parameter and the number of columns. In the second stage, among the Pareto front solutions, the set of solutions that belong to each cluster, analyzed according to their design variable such as P-parameter, coordinates of the points forming the surface, number of columns, seed, columns thickness, columns diameter, elements thickness, elements diameter and objective functions such as mass, displacement and elastic energy. In this phase, data set has 16 (13 design variable and 3 objective function) dimensions that it becomes increasingly difficult to make interpretations from the resultant data. Thus, PCA (Principal Component Analysis) before K-means clustering leads to reduced dimensions, which produces better visualizations of aggregated high-dimensional data. First, Standard Scaler was used to standardize the existing data and then PCA was conducted to fit the standardized data. Followed by that, the necessity of a solid decision on how many features must be kept based on the cumulative variance plot took place. On **Fig. 7**, the amount of variance captured (on the y-axis) depends on the number of components included (on the x-axis) is depicted. Empirically, the progressive result suggests preserving around 80 % of the variance in the process. So, in this instance, 3 components are kept.

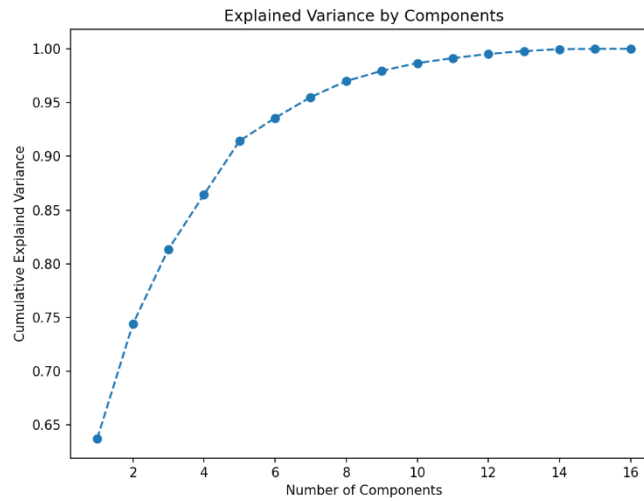


Fig. 7. Explained variance by components

This stage requires the number of clusters determination in a K-means algorithm. Running the algorithm with different numbers of clusters is one way to determine which number performs the best in terms of K. Therefore, the Within Cluster Sum of Squares (WCSS) approach was selected to examine data dissipation regarding the selected K. Based on the values of the WCSS and an approach known as the Elbow method, **Fig. 8** shows that after K=3, the graph with an Elbow Shape goes smoothly downward, thus this number would be a good suggestion for analyzing data. In this instance, the kink comes at the 3 clusters mark.

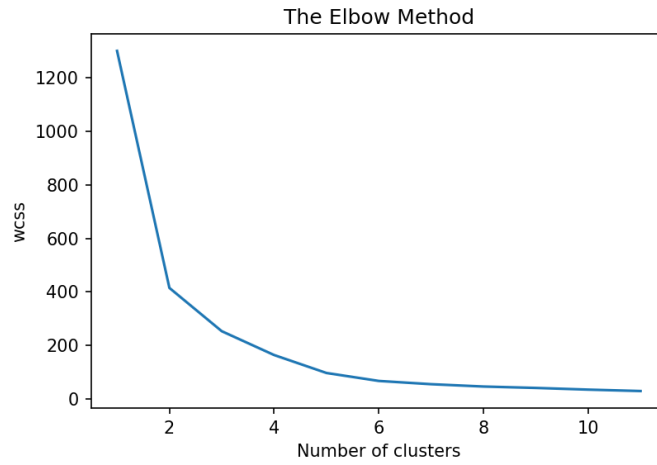


Fig. 8. The Elbow Method

3 Result

3.1 Decision-Making and Data Integration

Maintaining existential flexibility when making decisions regarding a project's conditional properties is essential since there are many variables to consider. Consequently, it is important to study design decisions when analyzing the results of any optimization procedure. Since all of the best-optimized designs are not superior to each other, based on the pareto optimal front of the NSGA-II process, the final design can be chosen from any of the best optimized solutions. As part of multi-objective optimization, there are various methods available for selecting the optimal solution from a pool of options on the optimal front. Some researchers believe an algorithmic process is necessary to select the final answer from the various options on the optimum front, including compromise programming, pseudo weight [35], and high trade-off points [36]. However, the architect may be able to contribute some perceptions regarding the project requirements to the selection of the most appropriate solution.

In this research project, the Thornton Tomasetti's Design Exploration platform is used to study the design iterations in a progressive yet comprehensive way. Design

Explorer is a platform that facilitates the selection of the best optimized solution for a particular project based on its attributes. As of this approach, **Fig. 9** (upper one) depicts all the optimal solutions in the optimum Pareto distribution. Throughout the polyline, the design solutions are associated with DVs and Objective Functions. In **Fig. 9** (lower one), the selection process was carried out in two steps using the design explorer. At the outset of the design process, Displacement and Elastic Energy were limited to a range of excellent values consistent with the designer's priorities and the project specifications. Initially, some solutions outside of the selected range were removed, leading to a selective removal step. In a subsequent step, the solution with the lowest mass was chosen.

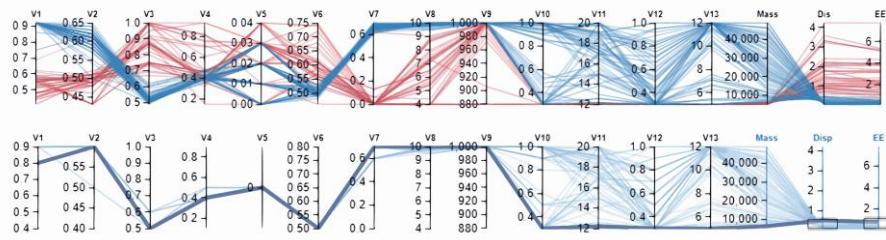


Fig. 9. Best Overall Selection Procedure

3.2 Optimization Result

In general, when the problem involves two objectives, Pareto front diagrams are well implemented for visualizing the multi-objective optimization process. therefore, the optimization process's output can be represented in two dimensions. Similar to this study, problems with three objective functions cannot be effectively illustrated in diagrams by the multi-objective optimization process. Therefore, it is suggested that using the authentic metric, “hypervolume Indicator” [37]. In evolutionary multi-objective optimization, the hypervolume indicator is a predetermined metric used to evaluate the effectiveness of search algorithms and guide the search [38]. According to **Fig. 11**, the graph for NSGA-II shows an upward growth generally, which increases where HV rises. On the basis of the diagram, it is obvious that during the optimization process, the algorithm's performance is quite satisfactory, and the objective functions are continuously improved. The growth in the function evaluations from 1 to 2500 is accompanied by a fluctuating rise in respect to the path of optimization, and from about 2500 onwards, it reaches a relative stability, which indicates that a much better result may not be possible.

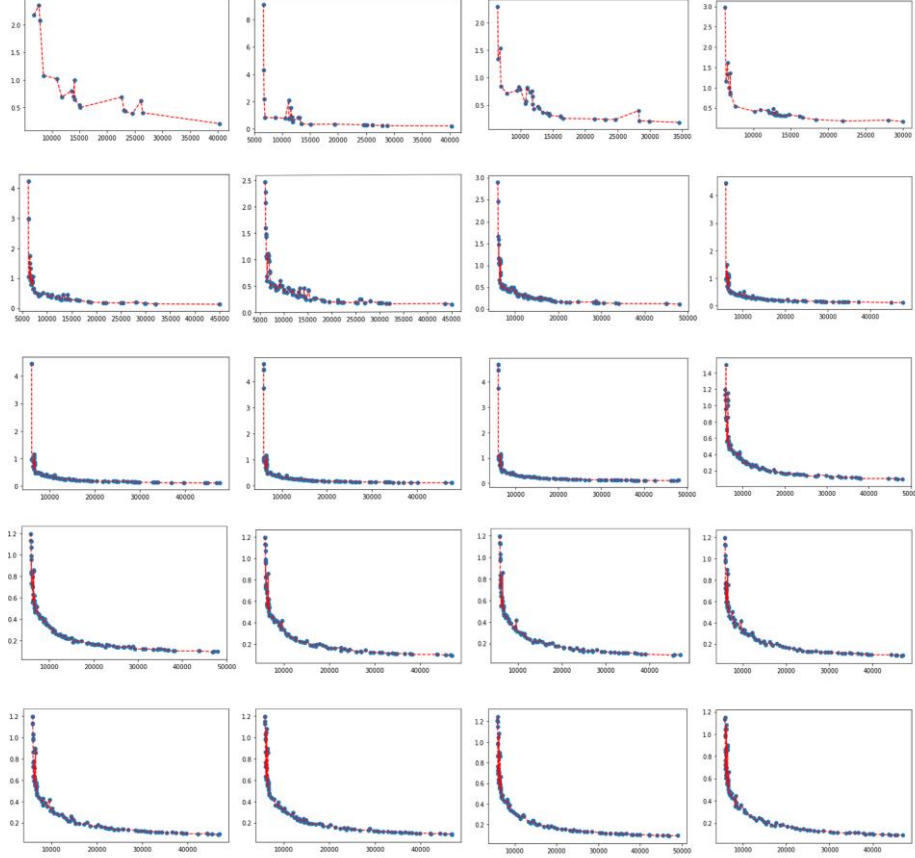


Fig. 10. One per five diagrams of Pareto-front during the optimization process from the latest 100 tries.

To delineate the pareto-front convergence during the optimization progression, one per five diagrams has been selected from the latest 100 tries. The set is shown in **Fig. 10**. According to part 2.2, the maximum Crowding distance will be selected based on different inputs. The loop continually finds the best solution based on the objective functions. After the model was optimized, the input and the output Data was accessible for further steps.

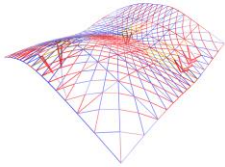
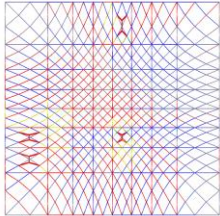
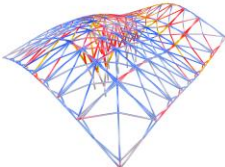
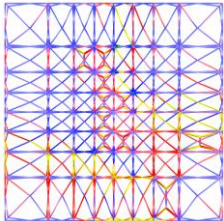
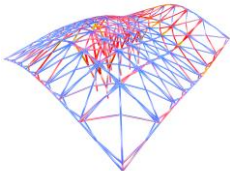
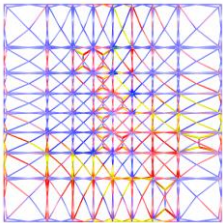
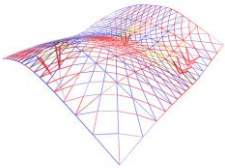
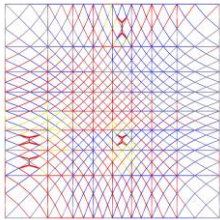
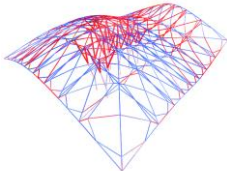
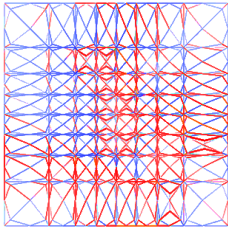
In the decision-making section, the Best Overall sample was selected as the most optimal solution for describing the performative design process within the workflow. Moreover, while the BO solution represents the design-to-analysis process in this study, other design scenarios also support data-driven decision-making. Best Displacement, Best Elastic Energy, and Best Mass are stages for comparing the results and identifying structural performance patterns relatively to a Diagrid structure where the P parameter equals 0.5 (Reference Case). Solutions with the highest performance in one component were selected from the optimal Pareto regardless of the other components attributes.

According to the Reference Case which provides the diagrid structure ($P = 0.5$), **Table 2** and **Table 3** outline four design scenarios. Inferred from the tables, the BD has a significant reduction in displacement (4.16 Cm) while its mass (43641.36 Kg) is higher than the Reference Case. BEE exhibits a mitigated elastic energy (7.59 kN/m) accompanied by an enhanced mass (36358.77 Kg), analogous to the Reference Case. There are no significant differences between the BM and the diagrid structure in terms of mass, displacement, and elastic energy. For the BO solution, the amount of Displacement, Elastic Energy and Mass in compare with Displacement in BD, Elastic Energy in BEE and Mass in BM increase by a certain amount (orderly, 0.41 Cm, 0.62 kN/m, 1197.33 Kg), while in comparison with Reference Case, Displacement and Elastic Energy decrease (3.75 Cm, 6.97 kN/m); nonetheless, Mass increases (1197.33 Kg). Thus, the BO solution seems having its displacement and elastic energy improved substantially. Regarding the Displacement attribute, the minimum displacement among the different scenarios is 0.08, which is 98.11% less than the displacement in the Reference Case (4.24 Cm), while this amount of displacement results an increasing amount in mass (18.64%) in the same scenario. For Elastic Energy, a minimum value of 0.17 kN/m represents 97.8% improvement over the Reference Case (7.76 kN/m). Even though the BO has a slightly higher Displacement and Elastic Energy than the BD and the BEE, it still has the least amount of Mass. Therefore, BO can be the best solution to reach an optimized structure among pareto optimal solution. Furthermore, it should be noted that the Column Thickness, Column Diameter, Elements Thickness, and Elements Diameter in the BO solution are equal to those in the Reference Case. Despite the fact that the number of columns in BO increases by ten, each randomly selected by the algorithm, whereas the Reference Case only has four columns. The BO performance appears to be more rational as compared to the diagrid for this reason. Considering the optimization setting, controlling the Mass beyond Displacement and Elastic Energy a more flexible fit to the design features. The workflow suggests that any other feature-based setting the designer may follow would produce similar progressive but analogous results.

Table 2. Summary of the Reference Case and four characteristic non-dominated solution

	Design Variable	Mas (Kg)	Displacement (Cm)	Elastic Energy (KN/m)
Reference Case	[0.5,0.48,0.87,0.47,0.03,0.62 ,0.4,972,0.3,12.07,0.3,5]	5224.17	4.24	7.76
Best Displacement	[0.9,0.61,0.51,0.41,0.02,0.49 ,0.68,10,1000,1,19.07,1,12]	48865.53	0.08	0.17
Best Elastic Energy	[0.9,0.59,0.51,0.41,0.02,0.49 ,0.68,10,1000,18.97,0.81,12]	41582.94	0.09	0.17
Best Mass	[0.5,0.48,0.87,0.47,0.03,0.62 ,0.4,972,0.3,12.07,0.3,5]	5224.17	4.24	7.76
Best Overall	[0.8,0.62,0.54,0.43,0.05,0.7 ,10,1000,0.3,12.19,0.3,5]	6421.5	0.49	0.79

Table 3. Comparison of the configuration of Reference and characteristic solutions

	Perspective	Plan
Reference Case		
Best Displacement		
Best Elastic Energy		
Best Mass		
Best Overall		

3.3 Clustering Result

The first stage involved visualizing the clusters in order to understand the characteristics of the features. **Fig.** on the left shows data clustering is constructed on three factors: Mass (Y-axis), Displacement (X-axis), and Number of Columns (Z-axis). The amount of mass is divided into three clusters: low, medium, and high, as indicated by the colors blue, red, and orange. Displacement of the grid shells is generally low in the green and yellow clusters. Displacement values, on the other hand, are not concentrated within the blue cluster and have been dispersed over a wide range. According to the results in the red and orange clusters, most of the data has a mass of medium or high, and the number of columns is nine or ten. There is a wide range of types of patterns with different P in the blue cluster, even though the majority of the data represent low mass.

Figure 12 on its right side, illustrates clustering of data based on three factors: Mass (Y-axis), Displacement (X-axis), and P parameter (Z-axis). Similarly, in the last stage, the three colors purple, red and orange are applied to identify low, medium, and high Mass. The analysis of P parameter reveals a consistent concentration across the iterations in the blue cluster, ranging from 0.4 to 0.5 and 0.8 to 0.9, indicating a low mass. In the red and orange clusters, where the mass is medium or high, the P parameter concentrations are mostly between 0.8 and 0.9. There is typically a small displacement and a medium or high mass associated with the red and orange clusters. In spite of the uniformity of the grid geometry in this cluster, the P parameter is 0.8 to 0.9, whereas the blue cluster, on the other hand, does not have a central standard deviation. It has a wide variety of patterns with an extensive range of P parameters and displacements with low mass.

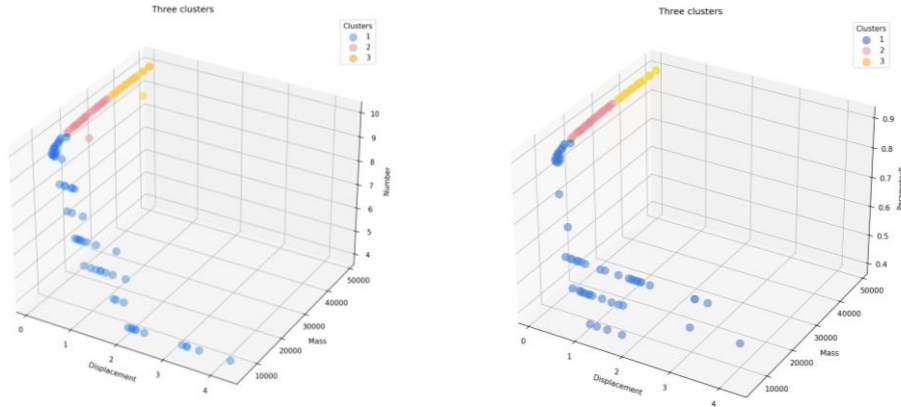


Fig. 11. Clustering in diverse format of aimed objectives

Due to the large number of potential coalitions between feature-based design settings, each specific set within every cluster is then analyzed in accordance with its design variables in the second stage. Therefore, with 16-dimensional dataset (13 design variables and 3 objective functions) it is increasingly difficult to interpret the findings. This phase hence, uses PCA (Principal Components Analysis) prior to applying K-means clustering in order to reduce the dimension of the data which results in improved visualizations of high dimensional dataset. In **Fig. 12**, the results of K-Means clustering are demonstrated with and without PCA.

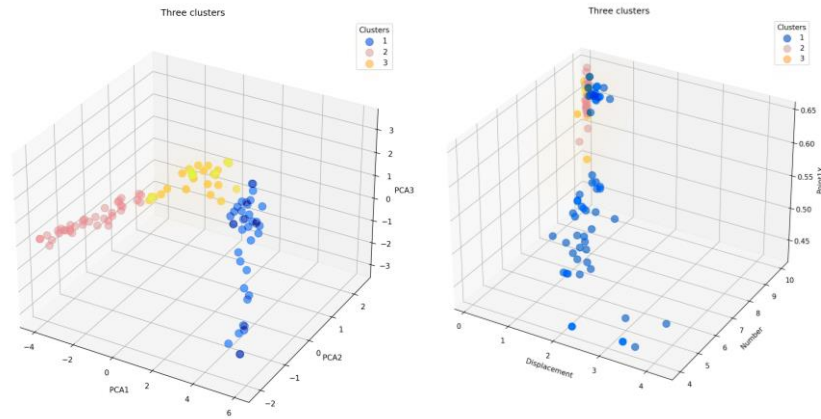
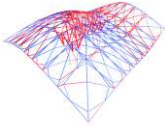
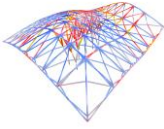
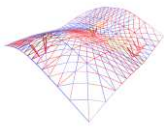
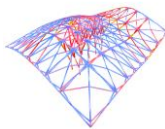


Fig. 12. Clustering with PCA (left) and, without PCA (right)

Following a more accurate clustering supported by PCA and analysis of the solutions obtained in the optimization section, summarized in **Table 4**, each solution is organized according to its specific cluster. Based on the structural free-form of each scenario, whether it is BM, BEE, BD, or even other scenarios, feature-based design scenarios can be developed. The data structure and the process, however, are managed in an Excel file that is supported by a cross platform functional algorithm, which is principally based on Grasshopper3D and Python. This allows for the input of desired design criteria and the output of a selection of data-driven design based on varying criteria from the designer. The Excel file stores the data from each design scenario, so that the designer can easily compare and analyze the different outcomes.

Table 4. Clustering of four characteristic non-dominated solutions

	Best Overall	Best Displacement	Best Mass	Best Elastic Energy
Free-Form				
Cluster	Cluster 3	Cluster 2	Cluster 1	Cluster 2
Design Variable	P parameter: 0.08 Number of Columns: 10 Columns Thickness: 0.3 Cm Columns Diameter: 12.19 Cm Element Thickness: 0.3 Cm Element Diameter: 5 Cm	P parameter: 0.9 Number of Columns: 10 Columns Thickness: 1 Cm Columns Diameter: 19.07 Cm Element Thickness: 1 Cm Element Diameter: 12 Cm	P parameter: 0.5 Number of Columns: 4 Columns Thickness: 0.3 Cm Columns Diameter: 12.07 Cm Element Thickness: 0.3 Cm Element Diameter: 5 Cm	P parameter: 0.9 Number of Columns: 10 Columns Thickness: 1 Cm Columns Diameter: 18.97 Cm Element Thickness: 0.81 Cm Element Diameter: 12 Cm
Objective Function	Mass: 6421.5 Kg Displacement: 0.49 Cm Elastic Energy: 0.79 kN/m	Mass: 48865.53 Kg Displacement: 0.08 Cm Elastic Energy: 0.17 kN/m	Mass: 5224.17 Kg Displacement: 4.24 Cm Elastic Energy: 7.76 kN/m	Mass: 41582.94 Kg Displacement: 0.09 Cm Elastic Energy: 0.17 kN/m

4 Conclusion

A novel and open-srouce research framework is presented in this paper that integrates structure and design, particularly for free-form shells with respect to spatial structures studies. The architecture of the framework is composed of three main phases: 1) generative design and modification, 2) optimization and selection, and 3) clustering and evaluation. In the course of the generative design procedure, a special type of Girih structure (Traditional yet functional geometry from Persian architecture) was selected that can be parametrized flexible while it could also encompass simple grid shell structures. The Iranian Chahar-Lengeh Girih has been examined in this regard, modeled and

analyzed for parametric performance with the Hankin method. Using Python, the optimization process is performed to minimize displacement, elastic energy, and mass in an integrated cross-platform including Grasshopper3D, Excel, Karamba3D and Machine Learning. As part of the ML algorithm implementation, K-Means is applied to free-form clustering in accordance with the feature-based design scenarios, by applying PCA to have the clustering set accurately. Therefore, by comparing iterations to the reference model with a P parameter of 0.5, which represents the diagrid shell, it has been inferred that a P parameter of 0.8 has resulted in an improvement in displacement and elastic energy of 88.44% and 89.82%, respectively, when it comes to finding the BO Solution. Despite the same thickness and diameter of the structural components, the BO alternative, which has only 0.05% mass above the diagrid shell, performs better in other attributes related to displacement and elastic energy. A conclusion of this study was that the reciprocal module on spatial structures applied to free-forms appears to be more effective if the objective functions and features are subjected to a large number of iterations in order to ensure there are interactions and reactions between a variety of factors, such as mechanical and physical characteristics. Future studies might also explore matching architectural planning to free-form structures with more flexible reciprocal geometries in both 2D and 3D formats as another strategy for incorporating more information into each iteration towards a more integrated model.

Replication of results

All Python codes, algorithms, and data utilized in this research, conducted in the Grasshopper3D and Jupyter Notebook environments, are available for public access on our open-source repository hosted on GitHub. We invite readers to access the codebase and implement the workflow by following this link: <https://github.com/Elhaaaam/Multi-Objective-Optimization-and-Machine-Learning>. This repository includes detailed documentation to facilitate the replication of our results and further exploration of the methodology.

References

- [1] H. Adeli and N. Cheng, "Integrated Genetic Algorithm for Optimization of Space Structures," *J. Aerosp. Eng.*, vol. 6, no. 4, pp. 315–328, 1993.
- [2] H. Adeli and N.-T. Cheng, "Concurrent Genetic Algorithms for Optimization of Large Structures," vol. 7, no. 1990, pp. 38–59, 1994.
- [3] H. Adeli and N.-T. Cheng, "AUGMENTED LAGRANGIAN GENETIC ALGORITHM FOR STRUCTURAL OPTIMIZATION By Hojjat Adeli, 1 Member, ASCE, and Nai-Tsang Cheng 2," *Aerospace*, vol. 7, no. 1, pp. 104–118, 1994.
- [4] A. Ehsani and H. Dalir, "Multi-objective design optimization of variable ribs composite grid plates," *Struct. Multidiscip. Optim.*, vol. 63, no. 1, pp. 407–418, Jan. 2021.
- [5] K. U. Bletzinger and E. Ramm, "Structural optimization and form finding of light weight structures," *Comput. Struct.*, vol. 79, no. 22–25, pp. 2053–2062, 2001.
- [6] M. Kociecki and H. Adeli, "Shape optimization of free-form steel space-frame

- roof structures with complex geometries using evolutionary computing,” *Eng. Appl. Artif. Intell.*, vol. 38, pp. 168–182, 2015.
- [7] Y. Sakai and M. Ohsaki, “Discrete elastica for shape design of gridshells,” *Eng. Struct.*, vol. 169, pp. 55–67, Aug. 2018.
 - [8] Y. Su, Y. Wu, W. Ji, and S. Shen, “Shape Generation of Grid Structures by Inverse Hanging Method Coupled with Multiobjective Optimization,” *Comput. Civ. Infrastruct. Eng.*, vol. 33, no. 6, pp. 498–509, Jun. 2018.
 - [9] J. Rombouts, G. Lombaert, L. De Laet, and M. Schevenels, “A novel shape optimization approach for strained gridshells: Design and construction of a simply supported gridshell,” *Eng. Struct.*, vol. 192, pp. 166–180, Aug. 2019.
 - [10] M. Kociecki and H. Adeli, “Two-phase genetic algorithm for size optimization of free-form steel space-frame roof structures,” *J. Constr. Steel Res.*, vol. 90, pp. 283–296, 2013.
 - [11] M. Kociecki and H. Adeli, “Two-phase genetic algorithm for topology optimization of free-form steel space-frame roof structures with complex curvatures,” *Eng. Appl. Artif. Intell.*, vol. 32, pp. 218–227, 2014.
 - [12] B. Gao, C. Hao, T. Li, and J. Ye, “Grid generation on free-form surface using guide line advancing and surface flattening method,” *Adv. Eng. Softw.*, vol. 110, pp. 98–109, 2017.
 - [13] R. Mesnil, C. Douthe, O. Baverel, and B. Léger, “Linear buckling of quadrangular and kagome gridshells: A comparative assessment,” *Eng. Struct.*, vol. 132, pp. 337–348, Feb. 2017.
 - [14] S. Dong, Y. Zhao, and D. Xing, “Application and development of modern long-span space structures in China,” *Front. Struct. Civ. Eng.*, vol. 6, no. 3, pp. 224–239, 2012.
 - [15] K. Deb, A. Pratap, S. Agarwal, and T. Meyarivan, “A fast and elitist multiobjective genetic algorithm: NSGA-II,” *IEEE Trans. Evol. Comput.*, vol. 6, no. 2, pp. 182–197, 2002.
 - [16] M. Pungale, Alberto, Sassone, “Morphogenesis and Structural Optimization of Shell Structures with the Aid of a Genetic Algorithm,” 2007.
 - [17] L. Iuspa and E. Ruocco, “Optimum topological design of simply supported composite stiffened panels via genetic algorithms,” *Comput. Struct.*, vol. 86, no. 17–18, pp. 1718–1737, 2008.
 - [18] P. Winslow, S. Pellegrino, and S. B. Sharma, “Multi-objective optimization of free-form grid structures,” *Struct. Multidiscip. Optim.*, vol. 40, no. 1–6, pp. 257–269, 2010.
 - [19] M. Bagheri, A. A. Jafari, and M. Sadeghifar, “Multi-objective optimization of ring stiffened cylindrical shells using a genetic algorithm,” *J. Sound Vib.*, vol. 330, no. 3, pp. 374–384, Jan. 2011.
 - [20] J. N. Richardson, S. Adriaenssens, R. Filomeno Coelho, and P. Bouillard, “Coupled form-finding and grid optimization approach for single layer grid shells,” *Eng. Struct.*, vol. 52, pp. 230–239, 2013.
 - [21] R. qiang Feng, L. Zhang, and J. ming Ge, “Multi-objective morphology optimization of free-form cable-braced grid shells,” *Int. J. Steel Struct.*, vol. 15, no. 3, pp. 681–691, Sep. 2015.
 - [22] V. G. Belardi, P. Fanelli, and F. Vivio, “Structural analysis and optimization of anisogrid composite lattice cylindrical shells,” *Compos. Part B Eng.*, vol. 139,

- pp. 203–215, Apr. 2018.
- [23] A. Ehsani and H. Dalir, “Multi-objective optimization of composite angle grid plates for maximum buckling load and minimum weight using genetic algorithms and neural networks,” *Compos. Struct.*, vol. 229, Dec. 2019.
 - [24] M. Goodarzi, M. Azimi, A. Mohades, and M. Forghani-Elahabad, “Effects of different geometric patterns on free form gridshell structures,” *Int. J. Electr. Comput. Eng.*, vol. 13, no. 2, pp. 1698–1707, Apr. 2023.
 - [25] C. Preisinger and M. Heimrath, “Karamba - A toolkit for parametric structural design,” *Struct. Eng. Int. J. Int. Assoc. Bridg. Struct. Eng.*, vol. 24, no. 2, pp. 217–221, 2014.
 - [26] Thornton Tomasetti, “Design Explorer.” 2020.
 - [27] J. MacQueen, “Some methods for classification and analysis of multivariate observations,” 1967.
 - [28] H. Abdi and L. J. Williams, “Principal component analysis,” *Wiley Interdisciplinary Reviews: Computational Statistics*, vol. 2, no. 4, pp. 433–459, Jul-2010.
 - [29] E. H. Hankin, *The Drawing of Geometric Patterns in Saracenic Art*. 1998.
 - [30] E. Hanbury Hankin, “Examples of Methods of Drawing Geometrical Arabesque Patterns,” *Math. Gaz.*, vol. 12, no. 176, pp. 370–373, 1925.
 - [31] E. H. Hankin, “Some Difficult Saracenic Designs. II. A Pattern Containing Seven-Ray Stars,” *Math. Gaz.*, vol. 18, no. 229, pp. 165–168, Oct. 1934.
 - [32] C. S. Kaplan, “Computer Graphics and Geometric Ornamental Design,” 2002.
 - [33] Z. Rashed Nia, “A Comprative Study of decoration and structural components Stucco Mihrab the Imamzada Rabi a Khatun of Oshtorjan with wooden pulpit Masjid-l Jami of Nain in the 8th Century AH.,” *Negareh Sci. Q. J.*, vol. 3, no. 59, p. 109, 2021.
 - [34] O. Veisi, A. Shakibamanesh, and M. Rahbar, “Using intelligent multi-objective optimization and artificial neural networking to achieve maximum solar radiation with minimum volume in the archetype urban block,” *Sustain. Cities Soc.*, vol. 86, Nov. 2022.
 - [35] K. Deb, *Multi-Objective Optimization using Evolutionary Algorithms*. 2001.
 - [36] L. Rachmawati and D. Srinivasan, “Multiobjective evolutionary algorithm with controllable focus on the knees of the pareto front,” *IEEE Trans. Evol. Comput.*, vol. 13, no. 4, pp. 810–824, 2009.
 - [37] E. Zitzler and L. Thiele, “Multiobjective Evolutionary Algorithms: A Comparative Case Study and the Strength Pareto Approach,” 1999.
 - [38] A. Auger, J. Bader, D. Brockhoff, and E. Zitzler, “Theory of the hypervolume indicator,” 2009, pp. 87–102.